BMJ Open Respiratory Research

Mapping regional strain in anesthetised healthy subjects during spontaneous ventilation

Pablo Cruces,[1,2] Benjamin Erranz,[3] Felipe Lillo,[1] Mauricio A Sarabia-Vallejos,[4] Pablo Iturrieta,[4] Felipe Morales,[1] Katherine Blaha,[5] Tania Medina,[2] Franco Diaz ,[2,3,6] Daniel E Hurtado[4,7,8]

To cite: Cruces P, Erranz B, Lillo F, *et al*. Mapping regional strain in anesthetised healthy subjects during spontaneous ventilation. *BMJ Open Resp Res* 2019;**6**:e000423. doi:10.1136/bmjresp-2019-000423

► Additional material is published online only. To view, please visit the journal online (http://dx.doi.org/10.1136/bmjresp-2019-000423).

Received 2 March 2019
Revised 17 September 2019
Accepted 9 October 2019

For numbered affiliations see end of article.

Correspondence to
Dr Franco Diaz;
francodiazr@gmail.com

ABSTRACT

Introduction Breathing produces a phenomenon of cyclic deformation throughout life. Biomechanically, deformation of the lung is measured as strain. Regional strain recently started to be recognised as a tool in the study of lung pathophysiology, but regional lung strain has not been studied in healthy subjects breathing spontaneously without voluntary or pharmacological control of ventilation. Our aim is to generate three-dimensional (3D) regional strain and heterogeneity maps of healthy rat lungs and describe their changes over time.

Methods Micro-CT and image-based biomechanical analysis by finite element approach were carried out in six anaesthetised rats under spontaneous breathing in two different states, at the beginning of the experiment and after 3 hours of observation. 3D regional strain maps were constructed and divided into 10 isovolumetric region-of-interest (ROI) in three directions (apex to base, dorsal to ventral and costal to mediastinal), allowing to regionally analyse the volumetric strain, the strain progression and the strain heterogeneity. To describe in depth these parameters, and systematise their report, we defined *regional strain heterogeneity index* [1+strain SD ROI(x)]/[1+strain mean ROI(x)] and *regional strain progression index* [ROI(x)–mean of final strain/ROI(x)–mean of initial strain].

Results We were able to generate 3D regional strain maps of the lung in subjects without respiratory support, showing significant differences among the three analysed axes. We observed a significantly lower regional volumetric strain in the apex sector compared with the base, with no significant anatomical systematic differences in the other directions. This heterogeneity could not be identified with physiological or standard CT methods. There was no progression of the analysed regional volumetric strain when the two time-points were compared.

Discussion It is possible to map the regional volumetric strain in the lung for healthy subjects during spontaneous breathing. Regional strain heterogeneity and changes over time can be measured using a CT image-based numerical analysis applying a finite element approach. These results support that healthy lung might have significant regional strain and its spatial distribution is highly heterogeneous. This protocol for CT image acquisition and analysis could be a useful tool for helping to understand the mechanobiology of the lung in many diseases.

Key messages

- Regional dynamic biomechanical characteristics of the lung have become the key to understanding its behaviour in health and disease.
- We successfully mapped the regional volumetric strain with advanced analysis of tomographic images, in subjects with uninjured lungs and spontaneous breathing.
- In these near-physiological conditions, we found highly heterogeneous lung parenchyma, which cannot be detected with standard methods.
- In addition, we evaluated regional volumetric lung strain in two time-points, proposing the strain heterogeneity index and strain progression index to standardise the regional strain report.

BACKGROUND

The lung can be described as a prestressed network of viscoelastic tissue elements deformed by surface tension. This characteristic allows the tissue to warp in a time-dependent manner on applied pressure and return to its initial configuration once the pressure is relieved.[1] Breathing produces a phenomenon of continuous cyclic deformation with each breath throughout life, where the applied pressure is inspiratory pressure. In biomechanical terms, the deformation of the lung attributable to tidal inflation is measured as strain. Strain for the whole lung (global strain) can be defined as the ratio between the tidal volume (V_T) and a reference volume, usually the volume at the end of passive expiration, which is known as the functional residual capacity (FRC). It is important to note that lung stress is the force developed on the lung structure (a surface unit) due to transpulmonary pressure. One unique characteristic of the lung tissue is that in its physiological state, the tissue is not unstressed because it is supported by transpulmonary pressure, even at the end of expiration.[2 3]

The transpulmonary pressure and the air compartments of the lung are not homogeneous, so the force (stress) applied to the lung is heterogeneous. Given these conditions, the regional strain of the lung is probably heterogeneous, but most of the current methods allow only quantification of global strain.

Mathematically speaking, the regional strain on a point of a deformable body is determined from the derivatives of the displacement field that deforms the body, that is, a function that maps points in a reference configuration to their corresponding locations in a deformed configuration. To describe the displacement field, deformable image registration techniques have been recently developed with successful applications in describing the motion of the lung.[4] Regional strain maps generated from image registration have recently started to be recognised as a tool in the study of lung pathophysiology. One advantage of these techniques is their non-invasive nature, which allows multiple time-points and several respiratory cycles of the whole lung to be studied.

Recently, three-dimensional (3D) biomechanical analysis based on finite-element techniques has been introduced to quantify regional lung strain from CT images.[5 6] Using this method, our group quantified regional strain in 11 human healthy subjects during a single full inspiration (total lung capacity) in supine decubitus, finding a significant effect of gravity on volumetric regional deformation.[6] Accurate measure of regional lung strain is relevant from a clinical standpoint, because strategies to reduce supraphysiological levels of global lung tidal deformation, that is, low V, driving pressure limitation, among others, are associated with better clinical outcomes in patients with and without lung injury.[7–10] Regional lung strain has been studied with the finite element method in subjects with healthy and acutely injured lungs. These studies have in common that measurements were during a single respiratory cycle and controlled ventilation, whether under mechanical ventilation or voluntary full inspiration.[5–7 11] Regional strain and heterogeneity are key concepts for studying the biomechanical characteristics of the lung in many diseases.[12–14] Measuring regional strain and heterogeneity changes over time during tidal ventilation is crucial to understand lung mechanobiology in physiological conditions.[14–17]

With these thoughts in mind, we designed this experimental study to generate 3D regional strain and heterogeneity maps of healthy rat lungs under spontaneous respiration. In addition, we wanted to evaluate if changes of lung regional volumetric strain could be quantified over time.

METHODS

Animal anaesthesia and monitoring

Six adult Sprague-Dawley rats were used for this study. In our animal research facility, the rats were maintained in a humidity-controlled, light-controlled and temperature-controlled environment before the experiment. Food and water were provided ad libitum.

After the inhalation anaesthetic induction with 2% isoflurane (Aesica Queenborough, UK), an intraperitoneal injection of ketamine (30 mg/kg, Drag Pharma Invetec) plus xylazine (5 mg/kg, Alfasan, Woerden-Holland) was administered. Inhalatory isoflurane (1.5%) was used during image acquisition. An adequate level of anaesthesia was administered and monitored with locomotor activity and the rodent anaesthetic score.[18] The subjects recovered and were placed in their boxes. Before the second image acquisition stage, an intraperitoneal injection of ketamine plus xylazine was administered. Fraction of inspired oxygen (FiO_2) was maintained at 100% during observation stage.

The rectal temperature, ECG readings, respiratory rate and oxygen saturation levels were monitored with a small animal physiological monitoring system (Holliston, Massachusetts, USA). Body temperature was maintained using an external heater. The room temperature was maintained at 25°C.

Image acquisition

Micro-CT (µ-CT) images were obtained from the subjects in a prone position after 10 min of clinical stability (T0). The subjects were placed in the prone position for recovery and monitored for 3 hours. This period was planned given the known time dependent consequences of anaesthesia in respiratory system physiology, that is, atelectasis, respiratory patterns and lung volumes.[19 20] A second µ-CT scan was performed (T3) after the observation period.

µ-CT images were acquired using a commercial SkyScan 1278 in vivo µ-CT scanner (Bruker microCT, Kontich, Belgium). This system has integrated a physiological monitoring device, which includes breathing movement and four-dimensional time-resolved microtomography capabilities. Dynamic scanning techniques, as used for the four-dimensional free-breathing µ-CT scanning protocol, exhibit the intrinsic problem of motion artefacts. We used a respiratory time-gating technique to reduce these artefacts. The motion of the animal's thorax was registered, and their breathing patterns were monitored to apply this procedure. The gating thresholds were set on these recordings. Scans were obtained using a source voltage of 70 kV and a current of 140 µA. The resolution was set to 50 µm. The retrospectively synchronised 'listmode' scan was performed with an exposure time of 40 ms, a scan rotation of 360° and a step of 0.75°. Twenty-five images were acquired per step for subsequent sorting into breathing cycle phases. The time of all video-recorded breathing inhalation movement maxima and the time of acquisition of all projection images were recorded during the scan in text files with a precision of ±1 ms to facilitate listmode sorting. End-expiratory and end-inspiratory gated and binned images around tidal breathing were further processed. The respiratory

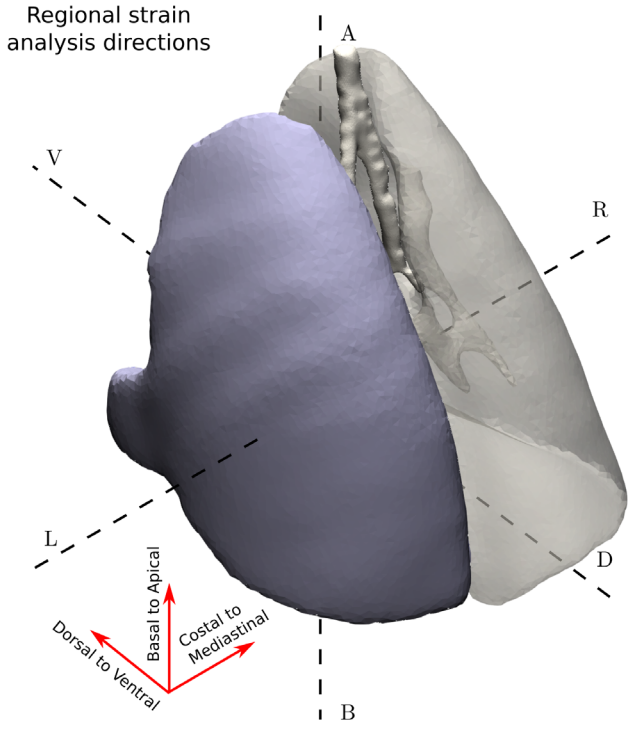

Figure 1 Three-dimensional sketch of the axes in which regional volumetric strain was measured with finite element method: apical to base, dorsal to ventral and costal to mediastinal.

wave train was displayed in real-time, and data were exported at the end of the scanning process for further reference. The entire scanning procedure took approximately 16 min. µ-CT images were then postprocessed by applying specific imaging filters to increase the signal-to-noise ratio and to enhance the contrast. The processes of image reconstruction, time sorting and image post-processing were achieved using the software provided by Bruker (NRecon, Tsort, DataViewer and CTAn). Subsequently, segmentation of the lungs was performed using the contour-active method implemented in the software ITK-Snap,[21] in which seeds are manually planted inside the lung domain. Those seeds begin to grow iteratively in the sectors with low greyscale gradients until reaching the edges where the gradient grows considerably. The final results of the image segmentation were always checked by clinical experts to ensure anatomically correct structures.

The segmented images were used to compute ventilatory parameters. The resulting masks allowed computing the end-of-inspiration lung volume (EILV) and end-of-expiration lung volume (EELV). FRC was assumed to be equal to EELV, and V_T during spontaneous ventilation was defined as V_T=EILV−EELV. Global strain was computed as V_T/FRC, and minute ventilation was defined as V_{min}=RR×V_T.

The animals were sacrificed at the end of the study by the intravenous administration of a lethal dose of thiopental (50 mg/kg, Richmond Laboratories, Buenos Aires, Argentina).

Biomechanical analysis and regional volumetric strain maps

The image-based biomechanical analysis was performed as previously described.[5 6] Basically, tetrahedral finite element meshes were used in the segmented masks of the lungs (left and right), the meshing process was carried out via the usage of the Computational Geometry Algorithms Library.[22] The finite element models were then subjected to a variational strain recovery method, which is employed to obtain a continuous approximation of the deformation gradient tensor field, from which the regional volumetric strain and principal stretch ratios are computed to obtain and visualise 3D maps of volumetric strain from the µ-CT scans at inspiration and expiration states.

The image registration procedure was performed using the package NiftyReg,[23] which generates continuous mapping for each point of the lung in expiration to its corresponding location in the inspiration image. This package finds an optimal transformation between these two µ-CT image sets by minimising a cost function that includes similarity measures and elastic regularisation (used to ensure the smoothness of the transformation). The online supplementary file shows a video of the sequential steps performed to obtain the 3D regional lung strain maps. These procedures allow us to generate a map of regional volumetric strain, from the expiration to the inspiration stage, which is indicative of local parenchymal deformation. We divided each lung domain into 10 isovolumetric regions of interest (ROIs) to compare the spatial distribution pattern of regional deformation in three directions: apex to base (AB), dorsal to ventral (DV) and costal to mediastinal (CM) directions (figure 1). Weighted mean and SD values of regional volumetric strain are computed for each ROI, where the sample includes tetrahedra contained in each ROI and weighting is performed according to each tetrahedron volume. The time evolution of the regional volumetric strain at each ROI was studied by means of the regional strain progression index (SPI), defined in formula (i):

(i) SPI=ROI(x)–mean strain at T3/ROI(x)–mean strain at T0.

An SPI=1 implies no changes, an SPI >1 is related to progression and an SPI <1 implies a reduction of regional strain over time.

To evaluate the dispersion of regional strain in an ROI, we defined the strain heterogeneity index (SHI), which corresponds to the coefficient of variation of the ROI strain distribution, expressed in terms of volumetric change. The SHI is expressed in formula (ii):

(ii) SHI ROI(x)=[1+strain SD ROI(x)]/[1+strain mean ROI(x)].

Statistical analysis

Data are expressed as the mean±SEM. To compare physiological respiratory data at the beginning and at the end of the experiment, we used Wilcoxon signed rank test. Analysis of variance was used to analyse the distribution

Table 1 Physiological respiratory data at the beginning (T0) and at the end of the study (T3)

Time	T0	T3	P value
SpO_2 (%)	98±1	99±1	0.99
RR (1/min)	95±10	100±16	0.01
V_T (mL/kg)	6.4±0.6	4.0±0.7	0.03
V_{min} (mL/kg/min)	604±66	418±93	0.12
FRC (mL/kg)	20.7±3.0	18.9±2.8	0.67
Global strain (%)	30.9±4.5	21.2±6.3	0.24

FRC, V_{min}, V_T and global strain were obtained from image analysis of µ-CT images. Wilcoxon signed rank test. P≤0.05 is considered significant.
µ-CT, micro-CT ; FRC, functional residual capacity; RR, respiratory rate; V_T, tidal volume.

of isovolumetric ROIs along the analysed axes (intragroup). The IBM SPSS software package (V.20.0; SPSS, Chicago, Illinois, USA) and GraphPad Prism V.5.0 (GraphPad Software, La Jolla, California, USA) were used for the statistical analyses. Significance was set at p<0.05.

RESULTS

The mean weight of the subjects was 285±8 g. All animals completed the experimental protocol.

Physiologycal measurements

During the first set of measurements, V_T and V_{min} were near physiological values. After the observation period, we observed a significant decrease in V_T and V_{min} in T3 compared with T0, without significant changes in FRC and global strain. Table 1 shows the respiratory variables and global calculated parameters from the µ-CT analysis at T0 and T3.

Regional strain distribution

When analysing the 3-axes regional lung strain distribution, we observed a significant gradient of regional lung strain over the AB direction at T0. The three upper ROIs in that axis had less regional strain than the mean. On the contrary, the two basal ROIs had higher regional strain compared with the mean. These differences disappear at T3. The regional lung strain distribution at T0 and T3

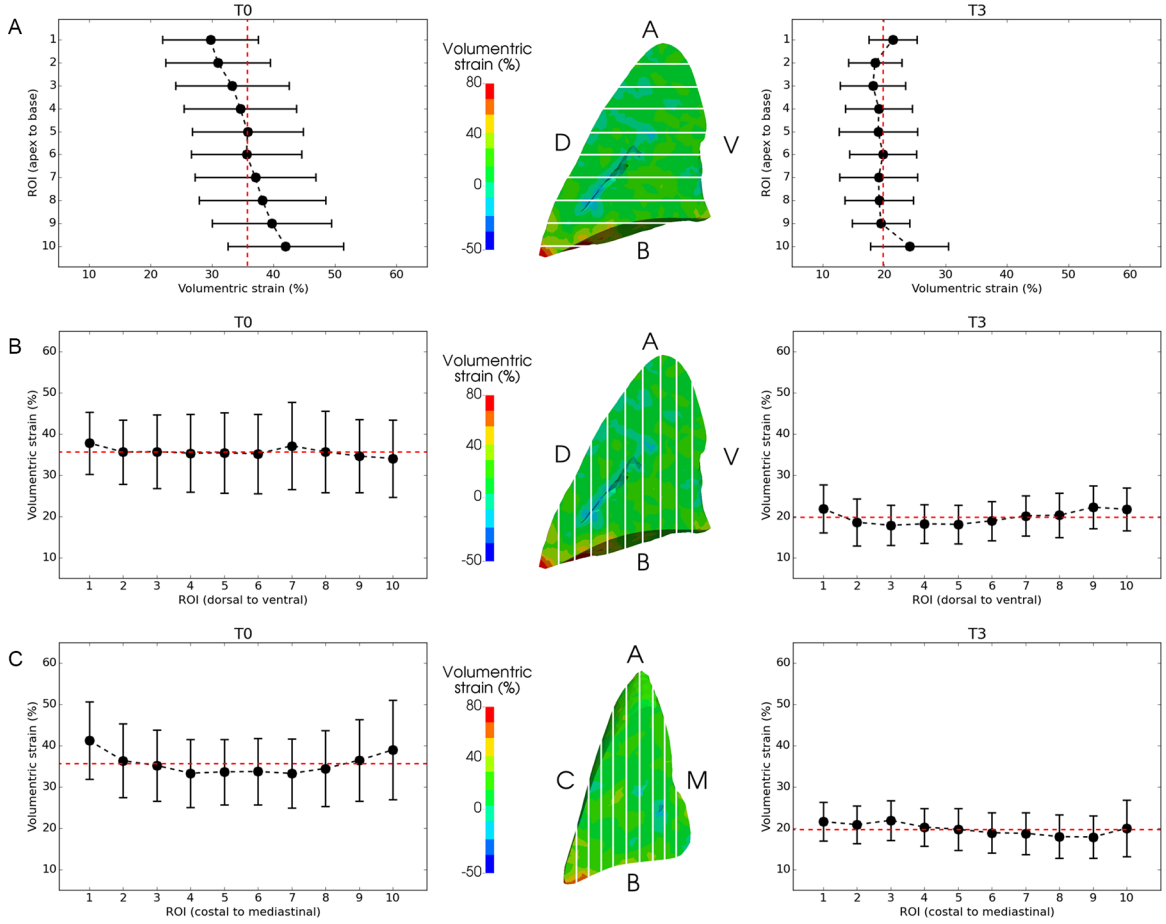

Figure 2 Regional strain of isovolumetric regions of interest (ROI) at T0 and T3 along apex to base (A), dorsal to ventral (B) and costal to mediastinal (C) axes. Data are shown as mean and SE. Dashed red line shows mean of the 10 isovolumetric ROIs along the axis.

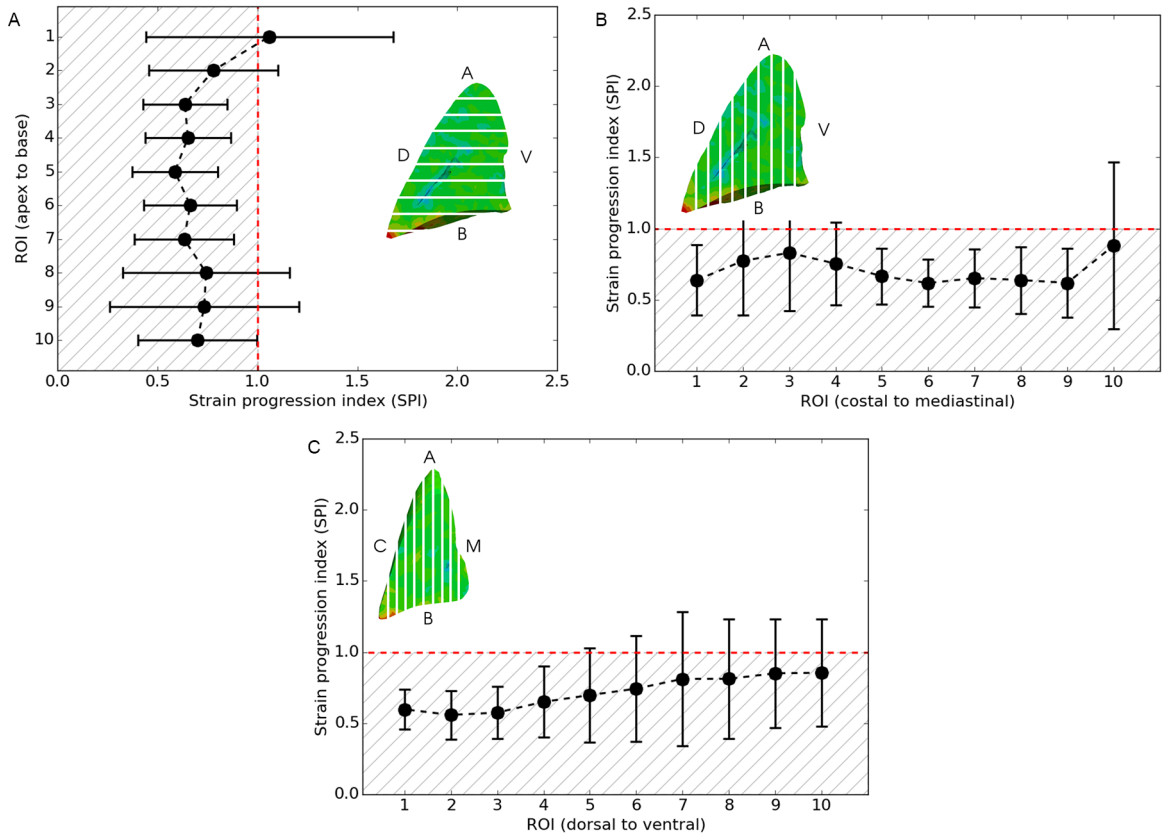

Figure 3 Regional strain progression index of isovolumetric regions of interest (ROI) at T0 and T3 along apex to base (A), dorsal to ventral (B) and costal to mediastinal (C) axes. Data are shown as mean and SE. Dashed red line shows mean of the 10 isovolumetric ROIs along the axis.

using AB, DV and CM ROIs subdivisions are reported in figure 2.

Regional strain progression

The distributions of regional SPI values along the AB, DV and CM directions are reported in figure 3. We observed a significant reduction in regional strain in 5 out of 10 ROIs in theAB direction, in 4 out of 10 in the ventral-dorsal direction and 6 out of 10 in CM axis.

Strain heterogeneity

The SHI values along the AB, DV and CM directions are reported in figure 4 at T0 and T3. Heterogeneity was frequent, between 30% and 40% in most analysed ROIs, but we did not find a specific pattern on the examined axes.

DISCUSSION

In this study, we successfully constructed 3D regional strain and heterogeneity maps of the lungs of anaesthetised healthy rats during spontaneous breathing at two time points. This is relevant because the finite element method allowed us to identify changes in regional pulmonary mechanobiology in the absence of primary pulmonary injury, in close to physiological conditions. Even in these conditions, finite element method is a sensitive tool to identify regional phenomena throughout the whole lung, confirming it as a breakthrough technique to study regional lung phenomena in many experimental scenarios.[4–6 11 12 14]

In our experiment, we found a regional strain gradient in the AB direction at the beginning of the observation period when analysing distribution of volumetric deformation across that axis. Regional strain in the apex was lower and in the base was higher compared with the mean. This gradient disappeared at the end of the observation period, when V_t was lower compared with the beginning. There was a reduction of region strain in most of ROIs, even when global strain measurements and FRC did not have significant changes. In addition, we identified heterogeneity of deformation in lungs without primary injury. It is important to highlight that this is a hot topic in respiratory physiology and pathophysiology, because heterogeneity of lung deformation was initially thought to happen only during disease. These regional differences cannot be measured with physiological or standard CT methods.

Changes in respiratory system parameters over time were expected to happen in this experimental model. We did not induce a primary lung injury, but anaesthetic drugs, like ketamine, xylazine and isoflurane, induces

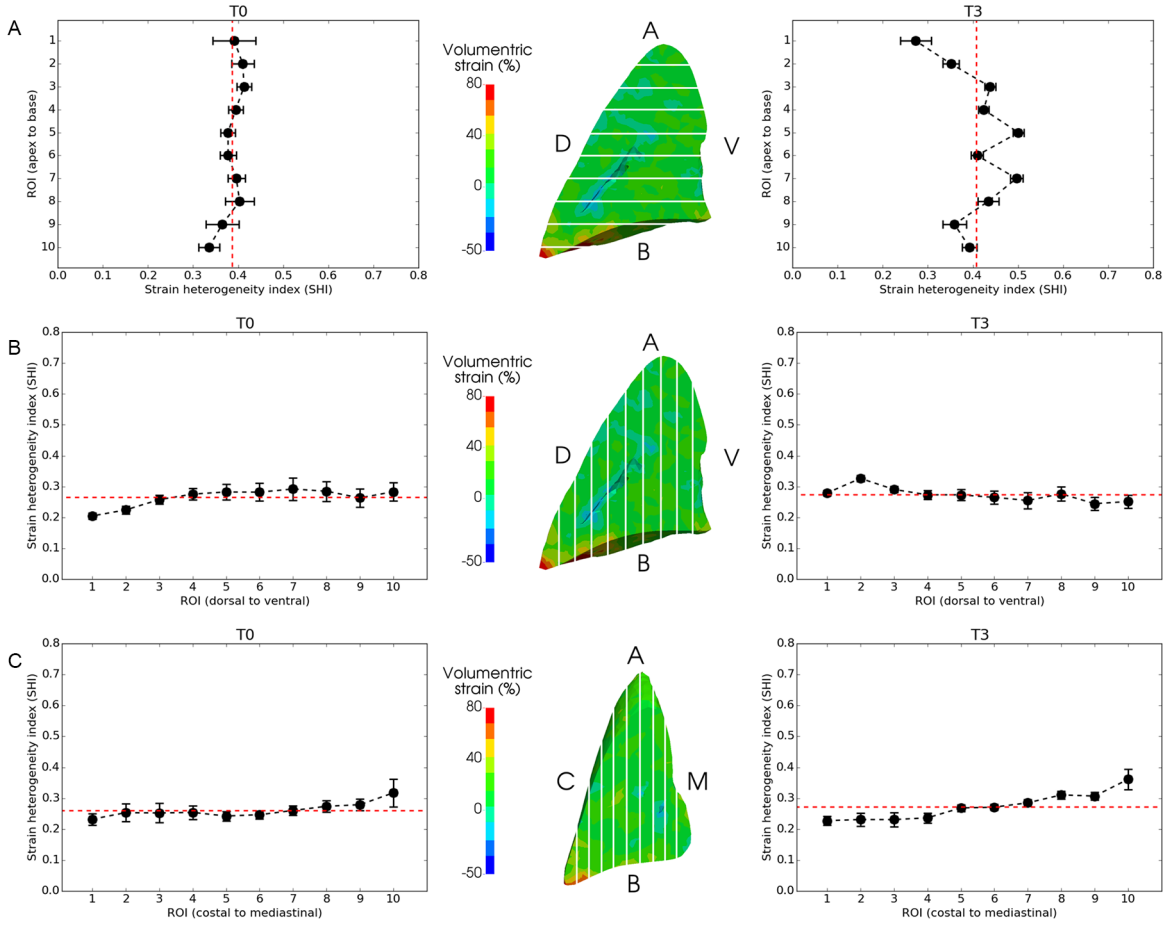

Figure 4 Regional strain heterogeneity index of isovolumetric regions of interest (ROI) at T0 and T3 along apex to base (A), dorsal to ventral (B) and costal to mediastinal (C) axes. Data are shown as mean and SE. Dashed red line shows mean of the 10 isovolumetric ROIs along the axis.

hypoventilation, specifically, a reduction in V_t.[24–28] The observed variation in regional strain during the observation period could be explained by this mechanism, even if FRC did not change. Another mechanism that can cause changes in respiratory system is FiO_2, which was set at 100%. This can cause time-dependent absorption atelectasis, which can lead to atelectrauma, one of the main factors of the shear stress due to cyclic opening and collapsing of the alveoli.[24 29] Overall, these effects of anaesthesia over time allowed us to make two measurements and compare their differences, reinforcing the non-invasive nature of this technique. To quantify the temporal evolution of regional deformation in the lung, we introduced the concept of regional SPI. Regional strain did not progress in our study, as SPI values in all ROIs were not significantly >1. To quantify this heterogeneity, we propose the concept of regional SHI, which allows us to characterise the inhomogeneities of regional deformations in the lung. We found that regional strain heterogeneity was between 30% and 40% in most ROIs in the three analysed axes and in the two time-points examined. This finding has particular translational relevance, as lung heterogeneity, measured in terms of regional differences in tissue aeration, has been related to stress risers and mortality in patients.[15] It is important to note that regional stress is related to regional strain by means of constitutive relations (regional elastance), and since regional strain can be directly estimated from the image-based biomechanical analysis, it may emerge as a better predictor of regional stress.[30]

Our findings might have an important translational impact on the understanding of regional lung deformation with perspectives that range from a description of advanced biomechanical mechanisms of lung injury to clinical implications to improve therapeutic strategies (ie, non-invasive ventilation and high flow nasal cannulas support respiratory failure) that might improve outcomes.

There is an increasing interest in regional strain, but at this moment the clinical and experimental data for its quantification are very limited. The most studied technique is electrical impedance tomography (EIT). EIT has many clinical advantages, but the information gathered with this method is partial, given the evaluation of a single segment of the lungs (ROI) in a single axis (DV). Also, the lung parenchyma analysed at the end of expiration is not the same area evaluated at the end of inspiration due to the caudal movement of the lungs generated by the excursion of the diaphragm muscle.[31] Measuring the volumetric regional lung deformation by finite element

method overcomes many of these limitations, but it is relatively new technique that is still under development. Nevertheless, we think that these results might also be used in future studies to report standardised regional lung strain, including isovolumetric ROI analyses, at least in two axes, and SHI and progression over time (SPI).

Our work suffers from certain limitations that should be improved in future experiments. Regional volumetric lung strain is a new research field, so a gold standard method for quantification and description has not been set. This does not allow us to compare our results with other methods. Given interference generated by metal artefacts during the acquisition of µ-CT images, animals could not be monitored by specific instruments, such as EIT or oesophageal pressure. As opnied out before, finite element approach in this field is a technique still under development, so high levels of radiation are currently needed for image acquisition. Also, there is a delay between the acquisition of images and the generation of strain maps. Also these limitations prevent its clinical use. However, future developments of this technique will probably allow identification of regional strain phenomena using low radiation protocols and automatised analysis for generation of these images in real time, all of which will open a field in many clinical settings. Despite these limitations, we highlight the novel nature of this work in quantifying the temporal changes in regional deformation from CT images in anaesthetised healthy subjects during spontaneous breathing.

In conclusion, it is possible to map regional lung strain and quantify heterogeneity and changes over time in healthy subjects during spontaneous breathing. Healthy lungs might have significant regional lung strain, and the strain is heterogeneous. Advanced CT image analysis, such as the one presented in this study, will help to understand the mechanobiology of the lung in many diseases. In the future, this method might help to evaluate the effect of therapeutic interventions, such as pharmacological treatments and respiratory support (ie, high flow nasal cannulas and mechanical ventilation).

Author affiliations
[1]Escuela de Medicina Veterinaria, Facultad de Ciencias de la Vida, Universidad Andres Bello, Santiago, Chile
[2]Pediatric Intensive Care Unit, Hospital El Carmen de Maipú, Santiago, Chile
[3]Facultad de Medicina Clínica Alemana, Universidad del Desarrollo, Santiago, Chile
[4]Pediatric Intensive Care Unit, Hospital Padre Hurtado, Santiago, Chile
[5]Pediatric Intensive Care Unit, Hospital Clínico La Florida Dra. Eloisa Diaz Insunza, Santiago, Chile
[6]Millennium Nucleus for Cardiovascular Magnetic Resonance, Santiago, Chile
[7]Institute for Biological and Medical Engineering, Schools of Engineering, Medicine and Biological Sciences, Pontificia Universidad Católica de Chile, Santiago, Chile
[8]Department of Structural and Geotechnical Engineering, School of Engineering, Pontificia Universidad Católica de Chile, Santiago, Chile

Acknowledgements The authors would like to thank the Plataforma Experimental Bio-CT, Faculty of Dentistry from Universidad de Chile (FONDEQUIP EQM150010), for performing the µ-CT analysis.

Contributors PC, BE and DEH are the guarantors of and take responsibility for the content of the manuscript, including the data and analysis. All authors have made substantial contributions to conception and design, or acquisition of data, or analysis and interpretation of data; drafted the submitted article or revised it critically for important intellectual content; provided final approval of the version to be published and have agreed to be accountable for all aspects of the work in ensuring that questions related to the accuracy or integrity of any part of the work are appropriately investigated and resolved. All authors have read and approved the manuscript.

Funding Fondo Nacional de Desarrollo Científico y Tecnológico grant (Fondecyt) # 1160631 to PC, BE and DEH.

Competing interests None declared.

Patient consent for publication Not required.

Ethics approval The study protocol was approved by the Universidad Andrés Bello Bioethics Committee, approval ID #05/2016 and #020/2017.

Provenance and peer review Not commissioned; externally peer reviewed.

Data availability statement All data relevant to the study are included in the article or uploaded as supplementary information.

ORCID iD
Franco Diaz http://orcid.org/0000-0003-4763-074X

REFERENCES

1 DuFort CC, Paszek MJ, Weaver VM. Balancing forces: architectural control of mechanotransduction. *Nat Rev Mol Cell Biol* 2011;12:308–19.
2 Loring SH, O'Donnell CR, Behazin N, *et al*. Esophageal pressures in acute lung injury: do they represent artifact or useful information about transpulmonary pressure, chest wall mechanics, and lung stress? *J Appl Physiol* 2010;108:515–22.
3 Talmor D, Sarge T, Malhotra A, *et al*. Mechanical ventilation guided by esophageal pressure in acute lung injury. *N Engl J Med* 2008;359:2095–104.
4 Murphy K, van Ginneken B, Reinhardt JM, *et al*. Evaluation of registration methods on thoracic CT: the EMPIRE10 challenge. *IEEE Trans Med Imaging* 2011;30:1901–20.
5 Hurtado DE, Villarroel N, Retamal J, *et al*. Improving the accuracy of Registration-Based biomechanical analysis: a finite element approach to lung regional strain quantification. *IEEE Trans Med Imaging* 2016;35:580–8.
6 Hurtado DE, Villarroel N, Andrade C, *et al*. Spatial patterns and frequency distributions of regional deformation in the healthy human lung. *Biomech Model Mechanobiol* 2017;16:1413–23.
7 Futier E, Constantin J-M, Paugam-Burtz C, *et al*. A trial of intraoperative low-tidal-volume ventilation in abdominal surgery. *N Engl J Med* 2013;369:428–37.
8 Brower RG, Matthay MA, Morris A, *et al*. Ventilation with lower tidal volumes as compared with traditional tidal volumes for acute lung injury and the acute respiratory distress syndrome. *N Engl J Med* 2000;342:1301–8.
9 Amato MB, Barbas CS, Medeiros DM, *et al*. Effect of a protective-ventilation strategy on mortality in the acute respiratory distress syndrome. *N Engl J Med* 1998;338:347–54.
10 Amato MBP, Meade MO, Slutsky AS, *et al*. Driving pressure and survival in the acute respiratory distress syndrome. *N Engl J Med* 2015;372:747–55.
11 Amelon R, Cao K, Ding K, *et al*. Three-Dimensional characterization of regional lung deformation. *J Biomech* 2011;44:2489–95.
12 Bodduluri S, Newell JD, Hoffman EA, *et al*. Registration-based lung mechanical analysis of chronic obstructive pulmonary disease (COPD) using a supervised machine learning framework. *Acad Radiol* 2013;20:527–36.
13 Wellman TJ, Winkler T, Costa ELV, *et al*. Effect of local tidal lung strain on inflammation in normal and lipopolysaccharide-exposed sheep*. *Crit Care Med* 2014;42:e491–500.
14 Retamal J, Hurtado D, Villarroel N, *et al*. Does regional lung strain correlate with regional inflammation in acute respiratory distress syndrome during nonprotective ventilation? an experimental porcine study. *Crit Care Med* 2018;46:e591–9.

15 Cressoni M, Cadringher P, Chiurazzi C, *et al*. Lung inhomogeneity in patients with acute respiratory distress syndrome. *Am J Respir Crit Care Med* 2014;189:149–58.
16 Motta-Ribeiro GC, Hashimoto S, Winkler T, *et al*. Deterioration of regional lung strain and inflammation during early lung injury. *Am J Respir Crit Care Med* 2018;198:891–902.
17 Gattinoni L, Marini JJ, Collino F, *et al*. The future of mechanical ventilation: lessons from the present and the past. *Crit Care* 2017;21:1–11.
18 Tsukamoto A, Konishi Y, Kawakami T, *et al*. Pharmacological properties of various anesthetic protocols in 10-day-old neonatal rats. *Exp Anim* 2017;66:397–404.
19 Kiss T, Silva PL, Huhle R, *et al*. Comparison of different degrees of variability in tidal volume to prevent deterioration of respiratory system elastance in experimental acute lung inflammation. *Br J Anaesth* 2016;116:708–15.
20 Ball L, Costantino F, Fiorito M, *et al*. Respiratory mechanics during general anaesthesia. *Ann Transl Med* 2018;6.
21 Yushkevich PA, Piven J, Hazlett HC, *et al*. User-guided 3D active contour segmentation of anatomical structures: significantly improved efficiency and reliability. *Neuroimage* 2006;31:1116–28.
22 CGAL. Computational geometry algorithms library. Available: http://www.cgal.org
23 Modat M, Ridgway GR, Taylor ZA, *et al*. Fast free-form deformation using graphics processing units. *Comput Methods Programs Biomed* 2010;98:278–84.
24 Wilding LA, Hampel JA, Khoury BM, *et al*. Benefits of 21% Oxygen Compared with 100% Oxygen for Delivery of Isoflurane to Mice (*Mus musculus*) and Rats (*Rattus norvegicus*). *J Am Assoc Lab Anim Sci* 2017;56:148–54.
25 Murat I, Chaussain M, Hamza J, *et al*. The respiratory effects of isoflurane, enflurane and halothane in spontaneously breathing children. *Anaesthesia* 1987;42:711–8.
26 Drummond GB. Breathing pattern during isoflurane anaesthesia with or without nitrous oxide. *Br J Anaesth* 1986;58:586–92.
27 Ford NL, McCaig L, Jeklin A, *et al*. A respiratory-gated micro-CT comparison of respiratory patterns in free-breathing and mechanically ventilated rats. *Physiol Rep* 2017;5:e13074.
28 Moriondo A, Marcozzi C, Bianchin F, *et al*. Impact of respiratory pattern on lung mechanics and interstitial proteoglycans in spontaneously breathing anaesthetized healthy rats. *Acta Physiol* 2011;203:331–41.
29 Duggan M, McNamara PJ, Engelberts D, *et al*. Oxygen attenuates atelectasis-induced injury in the in vivo rat lung. *Anesthesiology* 2005;103:522–31.
30 Gattinoni L, Protti A, Caironi P, *et al*. Ventilator-Induced lung injury: the anatomical and physiological framework. *Crit Care Med* 2010;38:S539–48.
31 Bachmann MC, Morais C, Bugedo G, *et al*. Electrical impedance tomography in acute respiratory distress syndrome. *Crit Care* 2018;22.